Journal of Applied Polymer Science

SiAlON-epoxy nanocomposite coatings: Corrosion and wear behavior

M. H. Moradi, M. Aliofkhazraei, M. Toorani, A. Golgoon, A. Sabour Rouhaghdam
Department of Materials Engineering, Faculty of Engineering, Tarbiat Modares University, Tehran, Iran
Correspondence to: M. Aliofkhazraei (E-mail: maliofkh@gmail.com or khazraei@modares.ac.ir)

ABSTRACT: In this study, epoxy powder as a matrix was combined with different contents of silicon–aluminum–oxygen–nitrogen (SiAlON) nanoparticles using a planetary ball mill. Pure epoxy and nanocomposite powders were applied on the surface of plain carbon steel components by the electrostatic spraying method. Curing of the coatings was done in an oven or microwave for the appropriate time. The coating structure and morphology of the SiAlON nanoparticles were studied by scanning electron microscopy and transmission electron microscopy, respectively. The corrosion properties of the coatings were assessed by immersion, Tafel polarization, and electrochemical impedance spectroscopy tests in 3.5% NaCl solution. The results show that addition of 10 wt % SiAlON nanoparticles markedly increases the corrosion resistance of epoxy coatings. Thus, it can be inferred that the corrosion rate of these coatings is 15 to 18 times lower than that of pure epoxy samples and 8 to 11 times lower than coatings with 20 wt % SiAlON. The higher corrosion resistance of nanocomposite coatings can be attributed to the barrier properties of SiAlON nanoparticles. The tribological performance of the coatings was studied with the pin-on-disk test. The results of wear testing show that the samples containing 10 wt % SiAlON provide about five times more wear resistance than pure ones and about two times more than coatings with 20 wt % SiAlON. However, the coefficient of friction for nanocomposite coatings is reduced about 50% compared to the pure sample. Also, the curing process in either regime (oven or microwave) has the same effect on the corrosion and wear properties, and the coatings are completely crosslinked. © 2016 Wiley Periodicals, Inc. J. Appl. Polym. Sci. **2016**, *133*, 43855.

KEYWORDS: coatings; friction; surfaces and interface; wear and lubrication

Received 11 November 2015; accepted 22 April 2016
DOI: 10.1002/app.43855

INTRODUCTION

Polymer coatings are some of the most commonly used coatings to protect against corrosion.[1] These coatings are characterized by their high strength, low weight, high thermal stability, and chemical resistance. Epoxy powder, one of the most widely used powder coatings, has good corrosion resistance in mild environments and mechanical properties such as fracture toughness (0.9 ± 0.1 MPa $m^{1/2}$) and impact strength (5.6 ± 0.7 K m^{-2}) as well as proper adhesion to the steel substrate.[2–4] Electrostatic spraying is among the easiest and least expensive methods of applying the powder coating. In this method, a high electric charge is needed for powder spraying.[5,6] The advantages of this method include low levels of waste of the powder and the uniformity of the coating film. The strength of polymers produced by this method is low compared to metals; thus, many efforts have been made to improve their corrosion and wear-resistance properties. The results of recent investigations show that the addition of nanoparticles to polymer-based coatings can improve mechanical properties such as their wear rate and enhance their capability of preventing the penetration of aggressive agents. In addition, increasing the corrosion resistance and reducing the wear rate can improve the performance of these coatings.[7–11] Alamri *et al.*[12] found that the addition of silicon carbide nanoparticles to an epoxy improves the mechanical properties of the coating. In another study, Palraj *et al.*[13] reported that the addition of silica nanoparticles improves both the corrosion resistance and the mechanical properties of the coatings, such as abrasion resistance and adhesive strength. Moreever, Piazza *et al.*[14] showed that the addition of montmorillonite clay nanoparticles to epoxy improves the thermal stability and the barrier properties of the coatings.

Silicon–aluminum–oxygen–nitrogen (SiAlON) is an advanced multifunctional ceramic that is crystallized in the Si-Al-O-N four-element system. Because of excellent physical properties such as high strength, toughness, and hardness and excellent resistance to thermal shock and corrosion, SiAlON can be used in antiwear and anticorrosion applications.[15–17] SiAlON is a combination of oxide and nonoxide ceramics. Nonoxide ceramics such as silicon nitride, because of their fracture strength properties and high thermal resistance, are suitable for high-temperature structural applications. Because oxide ceramics such as alumina show high corrosion resistance,

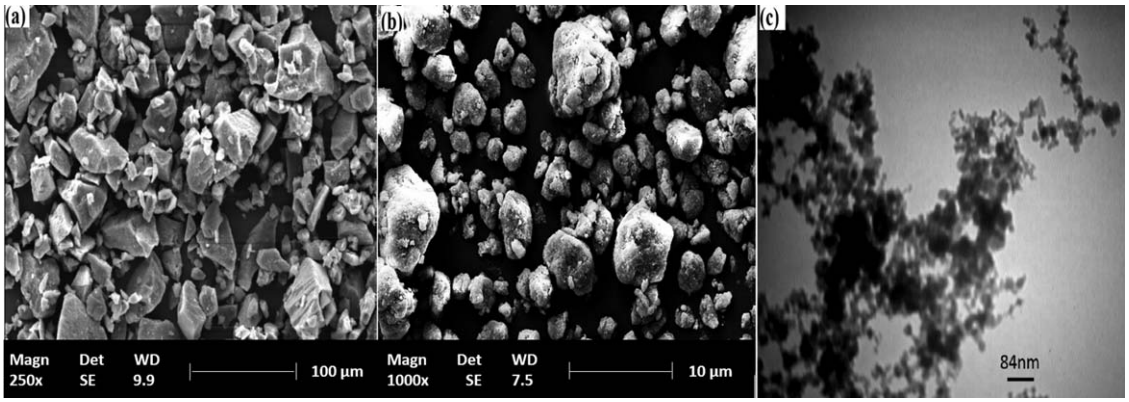

Figure 1. (a) SEM micrograph of the pure epoxy powder; (b) SEM micrograph of the nanocomposite powder after ball-milling; (c) TEM image of SiAlON nanoparticles.

SiAlON can exhibit a combination of satisfactory thermomechanical and chemical properties.[18,19] The β phase of SiAlON (β-SiAlON) is fabricated by sintering mixtures of Si_3N_4, Al_2O_3, AlN, and SiO_2 at temperatures above 1500 °C in N_2 atmosphere.[20]

The mixture and embedding type of nanoparticles with matrix powder coating are among the most important factors for determining the properties of the nanocomposite powder coating. Nanocomposite powder particles may become separated during spraying because of the differences in the properties of epoxy powder and nanoparticles (e.g., density, particle size, and electrostatic properties). Therefore, embedding of nanoparticles in powder coatings generally faces various problems. Thus far, various methods have been used to disperse nanoparticles in the powder coating. The planetary ball-milling technique is widely used for mechanical alloying of metals and the synthesis of nanostructured materials, intermetallic compounds, and amorphous structures. Recently, this technique was used to disperse nanoparticles within a polymer matrix.[21,22] It is believed that the high ductility of epoxy powder facilitates the dispersion of SiAlON nanoparticles in the field of epoxies.[18] In the present research, SiAlON nanoparticles were mechanically embedded in the epoxy resin matrix using a mechanical ball-milling process to produce a homogeneous nanocomposite powder.

SiAlON can exhibit a combination of nonoxide and oxide ceramic properties such as wear and corrosion resistance. Therefore, because of the complex properties of SiAlON nanoparticles, this nanoparticle can also enhance both the corrosion resistance and the wear resistance of polymer coatings.[15,18] The effect of adding SiAlON nanoparticles to an epoxy powder coating has not been studied yet. Therefore, this study was conducted to investigate the effect of adding SiAlON nanoparticles with a ball-milling technique to an epoxy powder on the improved protective and tribological properties of fabricated coatings.

In the present work, SiAlON nanoparticles were dispersed in an epoxy powder at 10 and 20 wt % using a mechanical ball-milling method. The fabricated nanocomposite powders were coated onto the surface of steel pieces by an electrostatic spraying method. The coatings were cured in either oven or microwave. The corrosion-resistance properties of the coated components were investigated using electrochemical impedance spectroscopic (EIS), Tafel polarization, and immersion tests. The results obtained show that the corrosion rate of coatings containing 10 wt % SiAlON is 15 to 18 times lower than that of pure epoxy samples. In order to investigate the wear behavior of the coatings, the pin-on-disk wear test was performed. The data obtained from the wear and friction tests reveal that the tribological properties of the coating are improved by the addition of SiAlON nanoparticles. Hence, the wear rate and coefficient of friction for nanocomposite coatings are decreased three to five times versus pure coatings. Furthermore, it was found that curing in oven or microwave has the same effect on the corrosion resistance and wear properties as the coatings are completely crosslinked in both regimes.

EXPERIMENTAL

Materials

Plain carbon steel sheets (0.02% C, 0.38% Al, 1.37% Si, 0.2% Mn, and the rest Fe) with the dimensions of $5 \times 6 \times 0.5\ cm^3$ were prepared and ground using 800- and 1200-grit emery papers in order to create the desired roughness on the surfaces, followed by surface degreasing by methanol. For final cleaning, the specimens were rinsed with distilled water and alcohol and dried at room temperature.

Epoxy powder (20–50 µm, NikfamGostar, Tehran, Iran) and β-SiAlON nanoparticles with a density of $3.3\ g\ cm^{-3}$ and hardness of 1430–1850 Kg mm^{-2} (10–30 nm, Reade Advanced Materials, East Providence, USA) were purchased. A transmission electron microscopy (TEM) image of the SiAlON nanoparticles is shown in Figure 1(c).

A proper mixture of epoxy powder and SiAlON nanoparticles (with 90/10 and 80/20 weight ratios) was conducted into the planetary ball mill with a ball-to-powder weight ratio (*B*/*P*) of 190:90 for 24 h to obtain a nanocomposite powder with the proper distribution of SiAlON nanoparticles in the epoxy matrix. Scanning electron microscopy (SEM) images of pure epoxy powder and nanocomposite powder after ball-milling are shown in Figure 1(a,b). To apply the coating on the surface of steel parts connected to ground, an electrostatic spraying device (IRIS Model, Tehran, Iran) with a Corona powder spray gun

Table I. Properties of Pure and Nanocomposite Coating Samples

Samples	Nanoparticle (wt %)	Cure
EC	—	Oven
EM	—	Microwave
ESC-10	10% nanoSiAlON	Oven
ESM-10	10% nanoSiAlON	Microwave
ESC-20	20% nanoSiAlON	Oven
ESM-20	20% nanoSiAlON	Microwave

and a 100 kV DC voltage source was used. After the coating process, two different conditions were considered for curing the coatings. In the first case, the specimens were placed in the oven for 12 min, and curing operations were performed at 200 °C (based on the results of differential scanning calorimetry (DSC) analysis). As the second case, the samples were cured in the microwave with a power of 900 W for 12 min (based on experimental observations). The properties of the coated pieces and their curing methods as well as their abbreviated names are shown in Table I.

Experimental Measurements

Measurements and Characteristics. The structure of SiAlON nanoparticles was studied using TEM (Zeiss, EMIOC, Germany). The filament voltage was fixed at 80 kV. The morphology of the epoxy powder and the morphology of the upper surface as well as cross sections of coatings were investigated using SEM (Philips XL30 model, Eindhoven, The Netherland). The thickness of coatings was measured with a Qnix 8500p portable device (Cologne, Germany) and by the cross section SEM images of the coatings.

Adhesion Test. Pull-off adhesion tests for pure and nanocomposite coatings were carried out with a Qualitest Positest (Lauderdale, USA) adhesion tester according to the ASTM D4541 standard. The test was repeated five times for each sample, and the results were reported as the mean and standard deviation. A field emission scanning electron microscope (FESEM; model MIRA3) equipped with mapping analysis was used to study the agglomeration of nanoparticles in the nanocomposite coatings.

Corrosion Properties. To investigate the corrosion-resistance properties of pure and nanocomposite powder coatings, immersion, Tafel polarization, and electrochemical impedance spectroscopy (EIS) tests were performed on the samples. In the immersion test, the potential of specimens was measured at different time intervals after immersion in 3.5% NaCl solution for 10,000 min. Finally, the graph of potential versus immersion time was drawn for each sample. Tafel polarization and EIS tests were performed on samples with an EG&G potentiostat/galvanostat (model 273A). All tests were conducted at the open circuit potential (OCP) and ambient temperature (25 °C). To carry out these tests, a three-electrode system including a saturated calomel reference electrode (SCE), a platinum electrode as the auxiliary electrode, and the samples immersed in a 3.5% NaCl solution as the working electrode were used. In the Tafel polarization test, the potential began to increase with a scan rate of 1 mV/s after 15 min of interruption. In this case, polarization was started from an initial potential of 250 mV below the OCP and continued up to 250 mV above the OCP. The data obtained from the Tafel polarization test was analyzed using Powersuite software. The polarization resistance (R_p) of the applied coatings was calculated using the equation $i_{corr} = \frac{\beta}{R_p}$,[23,24] where β is a constant and calculated using the following equation:

$$\beta = \frac{\beta_a \times \beta_c}{2.3(\beta_a + \beta_c)}$$

Where β_a and β_c show the Tafel slope of the anodic and cathodic branches in the polarization curve of each coating, respectively. In addition, the pore density was calculated using the equation $P \times D = \frac{R_{ps}}{R_p} \times 10^{\left(\frac{\Delta E}{\beta_a}\right)}$.[24,25] Here, R_{ps}, R_p, and ΔE are indicative of the polarization resistance of the steel substrate, the polarization resistance of the coating, and the potential difference related to the corrosion of coating and substrate, respectively.

To investigate electrochemical impedance, the EG&G potentiostat/galvanostat was coupled with a frequency response analyzer (FRA; Schlumberger Model 1250). During the EIS test, the frequency range varied from 10 mHz to 65 KHz, and the turbulence voltage was fixed at 10 mV. The effective area of the working electrode was 0.785 cm^2. To record and evaluate the data obtained from electrochemical impedance spectroscopy and fit them with the equivalent electrical circuits, Zview2 software was used.[26,27] The EIS test was repeated three times for each sample, and the results were reported as the mean and standard deviation.

Tribological Properties. Tribological tests were performed on the coated disk with a load of 10 N at room temperature (30% relative humidity) using the pin-on-disk wear test (52100 steel with a hardness of 64 HRC as a pin) according to the ASTM G99 standard. The test was conducted in a circular radial path of 1 cm at a constant linear speed of 0.05 m/s. Tribometer testing was performed for all samples based on a sliding distance of 10 m. The wear rate of each coating was finally calculated using the equation $W = \frac{m}{S \times F}$, where m, S, and F are the total weight loss (g), sliding distance (m), and load (N), respectively.[28] The pin-on-disk test was repeated three times for each sample, and the results for wear rate were reported as the mean and standard deviation.

RESULTS AND DISCUSSION

Microstructure of Coatings

As shown in Figure 2, the thicknesses of the pure epoxy and nanocomposite coatings produced are about 75 ± 7 μm. Considering the slight difference in thickness of the coatings produced, the effect of thickness changes on the protective and tribological properties of the coatings can be ignored. The coatings indicated relatively good densities. Besides, it seems that the coatings containing 10 wt % SiAlON have lower defects than the other specimens have. As can be seen, the pure and nanocomposite specimens containing 20 wt % SiAlON show low adhesion compared to the ESC-10 and ESM-10 samples. Cracks made in the samples show the weakness of their adhesion to the substrate and the loss of their protective and wear-resistance

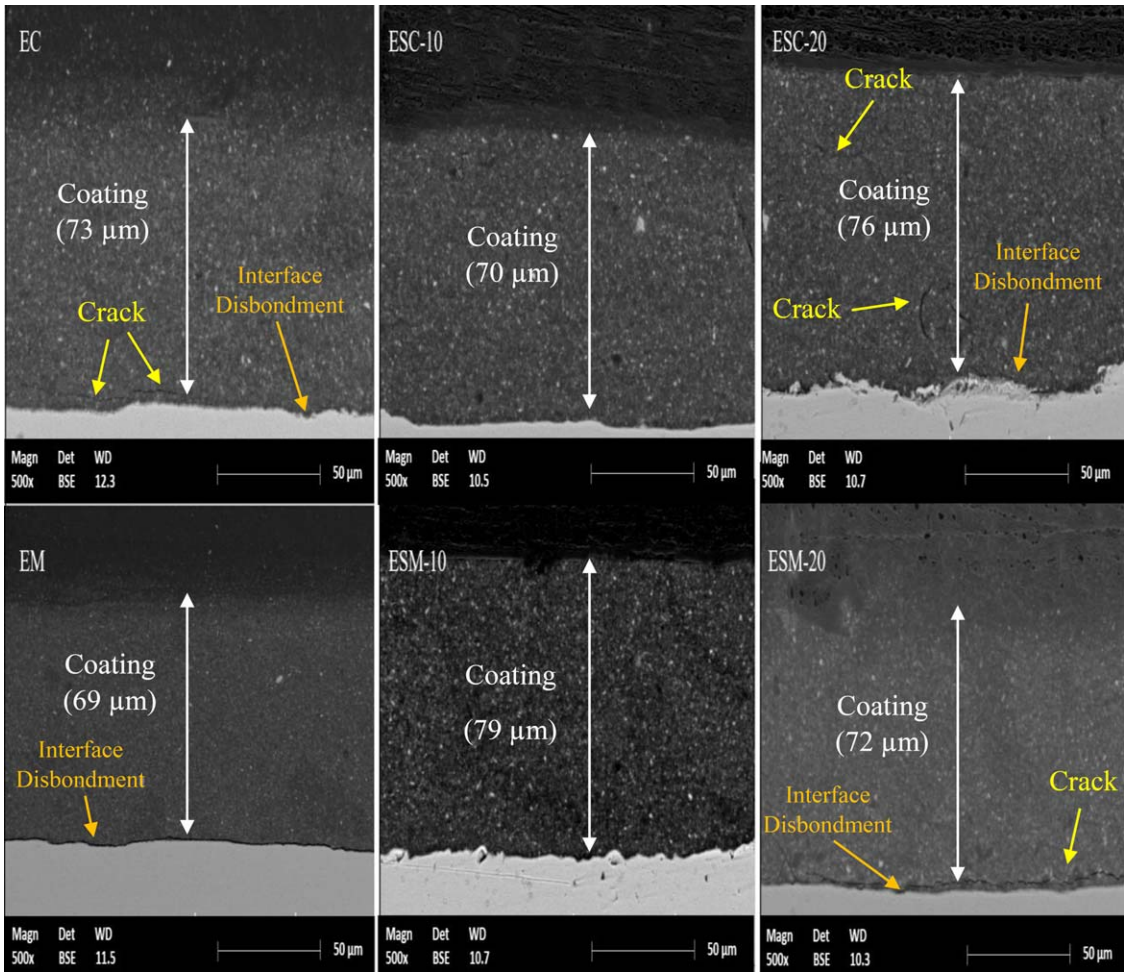

Figure 2. SEM images of cross sections of the coatings (pure epoxy and nanocomposite coatings with 10 wt % and 20 wt % SiAlON cured in oven or microwave) fabricated by electrostatic spraying. [Color figure can be viewed in the online issue, which is available at wileyonlinelibrary.com.]

properties.[29,30] Therefore, in some parts of the interface between coating and substrate, large cracks developed, and in some other parts, the coating was separated from the surface. As shown in the figure, the ESC-10 and ESM-10 samples indicate better interfaces between substrate and coating than in the other ones. It seems that the decrease in free volumes of the coatings by nanoparticles embedded in the polymer matrix leads to the increase in density and the coating–substrate interface. According to Hedayati *et al.*,[31] the existence of the cracks at the coating–substrate interface can be explained by crystallization of the coating. Residual stresses are developed that are due to the difference in the density of the amorphous phase and crystalline phase resulting from curing, producing cracks in the coating, particularly at the coating–substrate interface.[28,31,32] It might be assumed that the resulting residual stresses are large enough that they can cause cutting of the connection between the coating and substrate. To interpret the better adhesion of ESC-10 and ESM-10 coatings, the surface energy can be studied. Since metals have high surface energies compared to polymers, it is expected that polymers have a low tendency to adhere to a steel surface. The adhesion strength increases with the drop in the difference between the surface energies of polymer and steel.[28,33] According to Kisin *et al.*,[33] embedding of nanoparticles causes an increase in free energy that is due to the development of many interfaces with the matrix, resulting in a reduction of the free energy difference between steel and coating, as well as increasing the adhesion strength.[27,34] Adhesion test results (Table II) show that the ESC-10 and ESM-10 samples have higher adhesion strength than the other ones. It can be speculated that, in the case of the ESC-20 and ESM-20 samples, the positive effects of nanoparticles on increasing the amount of free energy have been decreased by the increased agglomeration of particles. Therefore, the ESC-20 and ESM-20 specimens have

Table II. Pull-Off Strength for Pure and Nanocomposite Coatings

Sample	Pull-off (MPa)
ESC-10	11.5 ± 5%
ESM-10	10.4 ± 6%
ESC-20	10.1 ± 3%
ESM-20	9.8 ± 5%
EC	8.5 ± 7%
EM	7.2 ± 6%

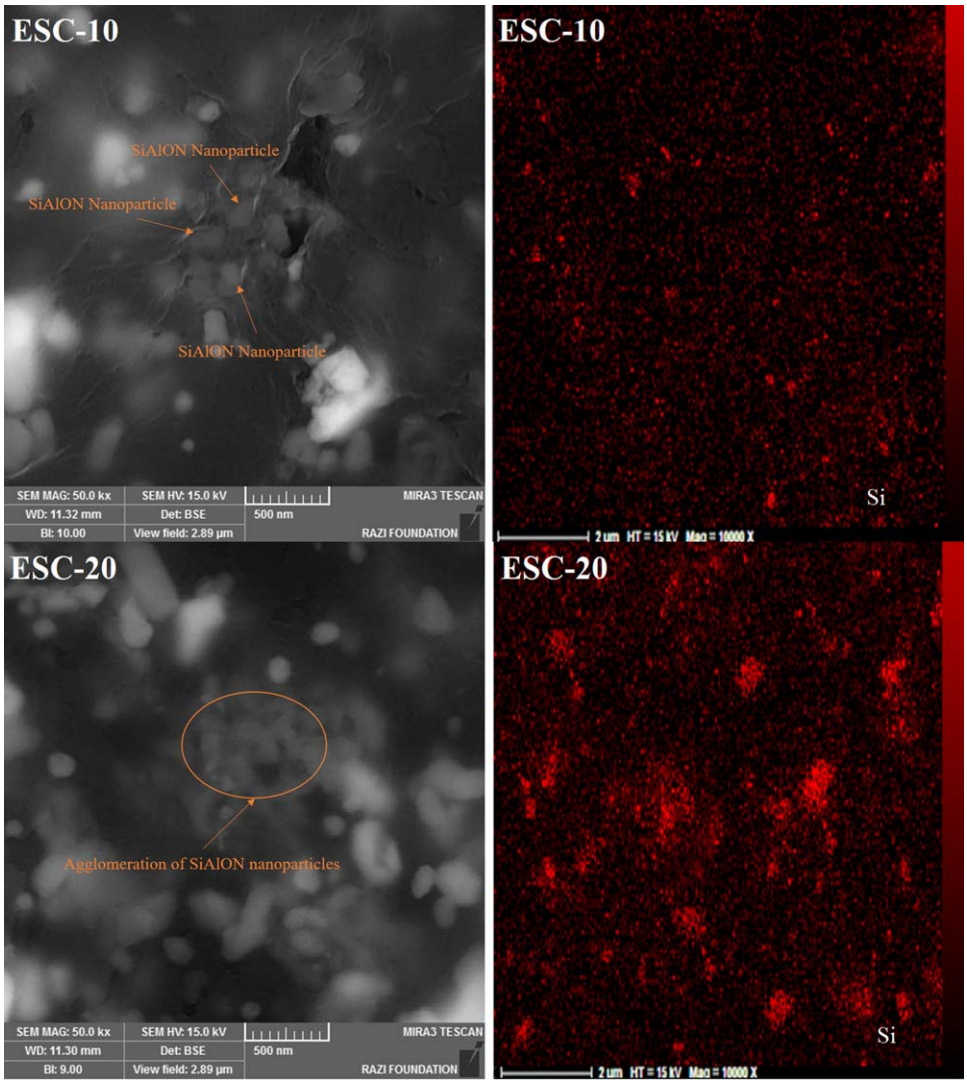

Figure 3. FESEM and mapping analysis from nanocomposite coatings with 10 wt % and 20 wt % SiAlON cured in an oven. [Color figure can be viewed in the online issue, which is available at wileyonlinelibrary.com.]

poor adhesion compared to the ESM-10 and ESC-10 ones. To prove the agglomeration of nanoparticles in coatings containing 20 wt % SiAlON, FESEM images with mapping analysis were used (Figure 3). As shown in Figure 3, the nanoparticles are largely agglomerated in coatings with 20 wt % SiAlON, and the nanoparticles in the coating with 10 wt % SiAlON are dispersed appropriately. The homogeneous, compact, and crack-free structure and the good adhesion to the metal substrate demonstrate the promising protective and tribological properties for ESC-10 and ESM-10 nanocomposite coatings.

SEM images related to the surface morphology of the formed coatings are shown in Figure 4. The figure clearly shows that the produced coatings include high-quality and properly aligned surfaces free from cracks and surface pores. The absence of cavities similar to volcanic craters, which is a characteristic of polymeric coatings, is indicative of a relatively good quality of coating.[35] The absence of cavities and surface cracks plays an important role in improving the wear-resistance and protective properties of the formed coatings.

Corrosion Behavior

Immersion Test. The penetration of corrosive agents such as H_2O, O_2, and H^+ ions into the substrate–coating interface leads to a consequent blistering, decrease of the adhesive bond strength, acceleration of cathodic reactions, and degradation of the coating and substrate.[36,37] The OCP values versus immersion time are shown in Figure 5. As can be seen, the OCP values increased for all samples by increasing the immersion time. The initial potential values of the pure and nanocomposite specimens were almost identical to each other and shift toward more active potentials (in the cathodic direction) with the passing of time. Also, the figure shows that the most favored behavior of resistance to the penetration of corrosive agents is found in the ESC-10 and ESM-10 specimens. Thus, except for an initial increase in the potential for 800 min after immersion, the

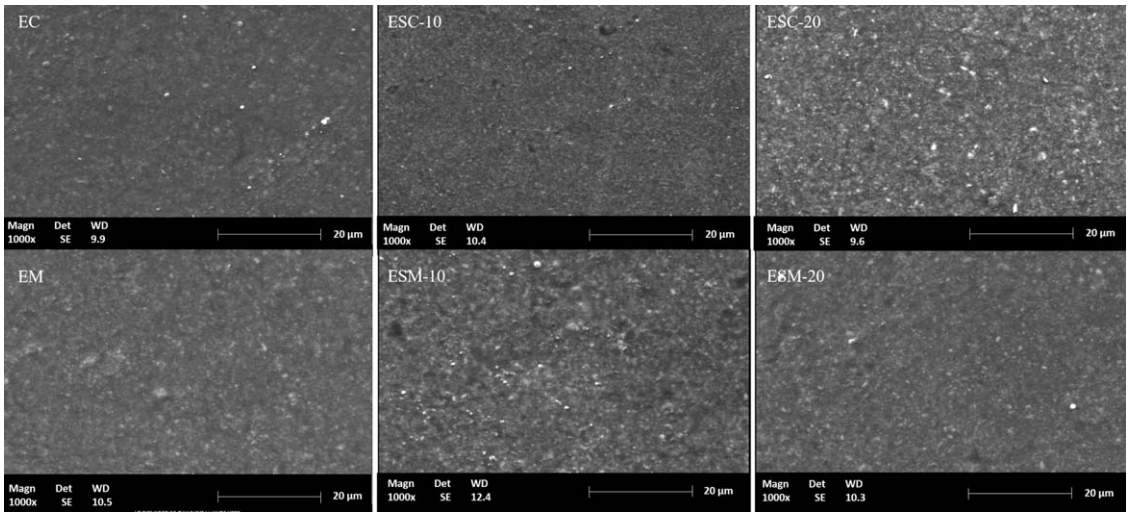

Figure 4. SEM images of the upper surface of pure epoxy coatings and nanocomposite coatings with 10 wt % and 20 wt % SiAlON cured in oven or microwave.

potential value remained almost constant during the remaining time of immersion. However, in the case of pure specimens, the OCP of the specimens is rising even 5000 min after immersion, which is indicative of continuous penetration of corrosive agents into the coating. The value of OCP for the ESC-10 specimen after almost 10,000 min of immersion is about 113 mV lower than that of the pure specimen under the same curing conditions. The penetration of electrolyte and corrosive ions through defects and voids in the coating increases the OCP values for the tested samples.[38] It seems that the presence of nanoparticles embedded in the ESM-10 and ESC-10 specimens has resulted in control of the penetration level of corrosive agents and improvement in the protective performance of the aforementioned coating.

The general behavior of potential changes in coating samples mainly consists of an initial rapid rise, followed by a more slow increase and a high rate of increase thereafter. This three-step behavior reflects different stages of electrolyte penetration through the organic coating.[29,30,39] The initial entrance of the corrosive solution into the coating considerably increases the OCP values for all coatings.[29,40] For instance, the OCP value for the pure coating cured in the oven reaches from −510 mV vs. SCE to −634 mV vs. SCE after about 1200 min of immersion. The first stage finishes in 1200 min of immersion for all specimens. As can be seen, the increase in the OCP for pure specimens is higher than that of the nanocomposites samples. After the initial stage, the values for pure specimens as well as the ESC-20 and ESM-20 samples move with a slope less than that of the initial step toward more noble OCP values. However, the ESC-10 and ESM-10 samples exhibit almost constant potentials for 10,000 min of immersion. The drop in the slope related to the increase in OCP values can be explained by plugging of the cavities with corrosion products.[29,30] Usually, if the corrosive solution is able to dissolve or dispose of corrosion products within the pores, the value of OCP increases again.[30]

Considering the lack of a third region for the ESC-10 and ESM-10 specimens, it can be concluded that longer immersion times are needed in order to create this region.[30] The potential rise in the case of other samples is shown in Figure 5. Thus, after filling the voids in the coating with corrosion products, the potential rise decreases (second region); however, the dissolution of corrosion products proceeds, and the aforementioned growing process continues at a high rate again. This trend is completely clear for pure samples. For example, the EC specimen entered the third region after 4000 min of immersion and was faced with a sharp increase in the potential. Nevertheless, the ESM-10 and ESC-10 samples do not enter the third region even after 10,000 min.

It can be speculated that the morphology of nanocomposite coatings is denser than that of pure coatings because the free volume is occupied by nanoparticles. Therefore, samples containing nanoparticles show better corrosion-protection performance compared to the pure ones. Hence, as Hosseini *et al.* also concluded, a longer time is required for the corrosive solution to have access to the coating–substrate interface.[30] Thus, nanocomposite coatings retain their adhesion to the substrate for a longer time. An increase in weight percent of nanoparticles from 10 to 20 adversely affected the protective performance of the coatings. In other studies, a similar result for the effect of an increase in the weight percent of nanoparticles on the protective performance of the coatings was reported.[41]

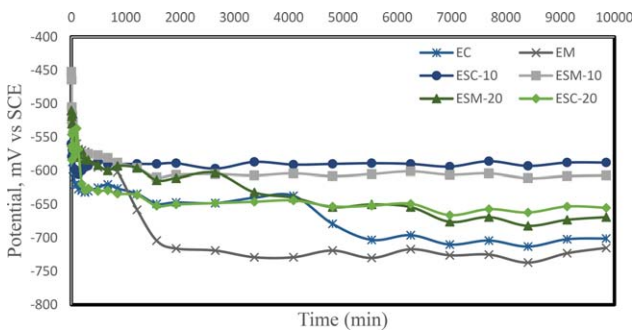

Figure 5. Open circuit potential changes for pure and nanocomposite coatings in immersion test. [Color figure can be viewed in the online issue, which is available at wileyonlinelibrary.com.]

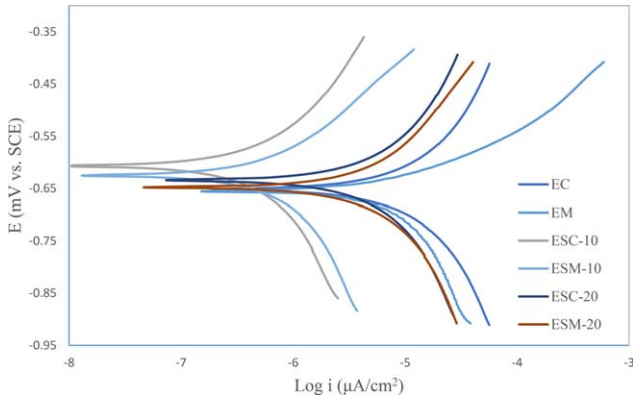

Figure 6. Tafel polarization curve for coated samples (pure epoxy coatings and nanocomposite coatings with 10 wt % and 20 wt % SiAlON cured in oven or microwave). [Color figure can be viewed in the online issue, which is available at wileyonlinelibrary.com.]

It can be concluded that embedding of SiAlON nanoparticles into the epoxy matrix leads to an increase in the blocking effect and the effective diffusion path length for water molecules.[41,42] Therefore, the penetration and absorption of water and corrosive molecules are greatly reduced, resulting in a decrease in the amount of damage and an increase in the shelf life of the coatings. It can be stated that the presence of nanoparticles in the matrix increases the access path for penetration of the corrosive molecules and, therefore, decreases the possibility of the penetration of corrosive molecules.[43] As a result, nanocomposite coatings seem to have denser structures than pure ones, leading to much less penetration of the corrosive agents.[43]

Tafel Polarization Test. The Tafel polarization test was carried out on pure and nanocomposite samples in 3.5% NaCl solution. Behavioral changes of potential vs. current are illustrated in Figure 6 for various samples. The data obtained by extrapolation of the Tafel diagrams using Powersuite software, such as corrosion potential (E_{corr}), corrosion current density (i_{corr}), R_p, and $P \times D$, are listed in Table III. In this table, the bare metal is metal without a coating. From a kinetics point of view, lower corrosion rate and corrosion current density reflect less tendency to corrode. On the other hand, from a thermodynamic perspective, a more noble corrosion potential reflects less tendency to corrode.[44,45]

According to the results obtained from the Tafel test, as well as the data given in Table III, the ESC-10 and ESM-10 samples have low corrosion rate (0.25 mpy for ESC-10 and 0.36 mpy for ESM-10) and corrosion current densities (0.42 μA/cm^2 for ESC-10 and 0.62 μA/cm^2 for ESM-10) in comparison to the samples containing 20 wt % SiAlON and pure specimens. Hence, it can be concluded that the ESM-10 and ESC-10 samples have good corrosion-resistance performance compared to other samples. For instance, by adding 10 wt % SiAlON to the coating samples, the corrosion rate decreased 15 to 18 times from that of pure samples.

As shown in Table III, the results related to the density of the pores show that presence of SiAlON nanoparticles leads to a decrease in the $P \times D$ value. The denser structures of the ESC-10 and ESM-10 samples, as well as their lower pore numbers compared to pure samples and coatings containing 20 wt % SiAlON, can also be predicted by an immersion test. It seems that the presence of nanoparticles and their barrier properties improve the blocking behavior of nanocomposite samples against the penetration of electrolyte compared to the pure samples.[24] The results derived from the Tafel polarization test confirm the immersion test outputs and show that the embedding of nanoparticles decreases the number of pores in coatings and increases the density and penetration path of corrosive molecules through the coating. Furthermore, the polarization resistance (R_p) of the ESC-10 and ESM-10 samples is much higher for these samples compared to that of the remaining samples.

According to the results derived from the Tafel polarization test, the type and conditions of curing for samples cured in either oven or microwave are appropriate, so the curing type has almost no impact on the protective properties of the coatings. As can be seen, samples cured in the oven show slightly better protective performance than those cured in the microwave; however, there is no substantial difference between these two curing regimes. Because the crystallization level and the strength of film chains influence the penetration of an electrolyte solution,[46] and considering that the results derived from similar samples cured in either oven or microwave exhibit almost similar protective behaviors, it can be concluded that the crosslinking density was almost equal for both regimes. Furthermore, from the curing condition point of view, polymeric networks form with a similar percentage of crystallinity and strength of chains in either case (oven or microwave).

The increase in weight percentage of nanoparticles from 10 to 20 wt % adversely affected the increase in the protective performance of the coating samples. The tendency of nanoparticles

Table III. Data Obtained from Tafel Polarization Test Using Powersuite Software

Sample	$E_{I=0}$ (mV vs. SCE)	i (μA/cm^2)	$\beta_{cathodic}$ (mV/decade)	β_{anodic} (mV/decade)	Corrosion rate (mpy)	R_p (Ω cm^2)	$P \times D$ (%)
EC	−653	7.78	219	210	4.54	4.70	0.11
EM	−665	9.25	365	122	5.4	3.37	0.10
ESC-10	−608	0.43	272	210	0.25	94.06	0.026
ESM-10	−630	0.62	357	372	0.36	100.28	0.011
ESC-20	−629	4.76	227	181	2.18	9.19	0.130
ESM-20	−646	5.01	269	247	2.92	8.77	0.07
Bare	−634	26.22	596	66	12.01	0.98	1

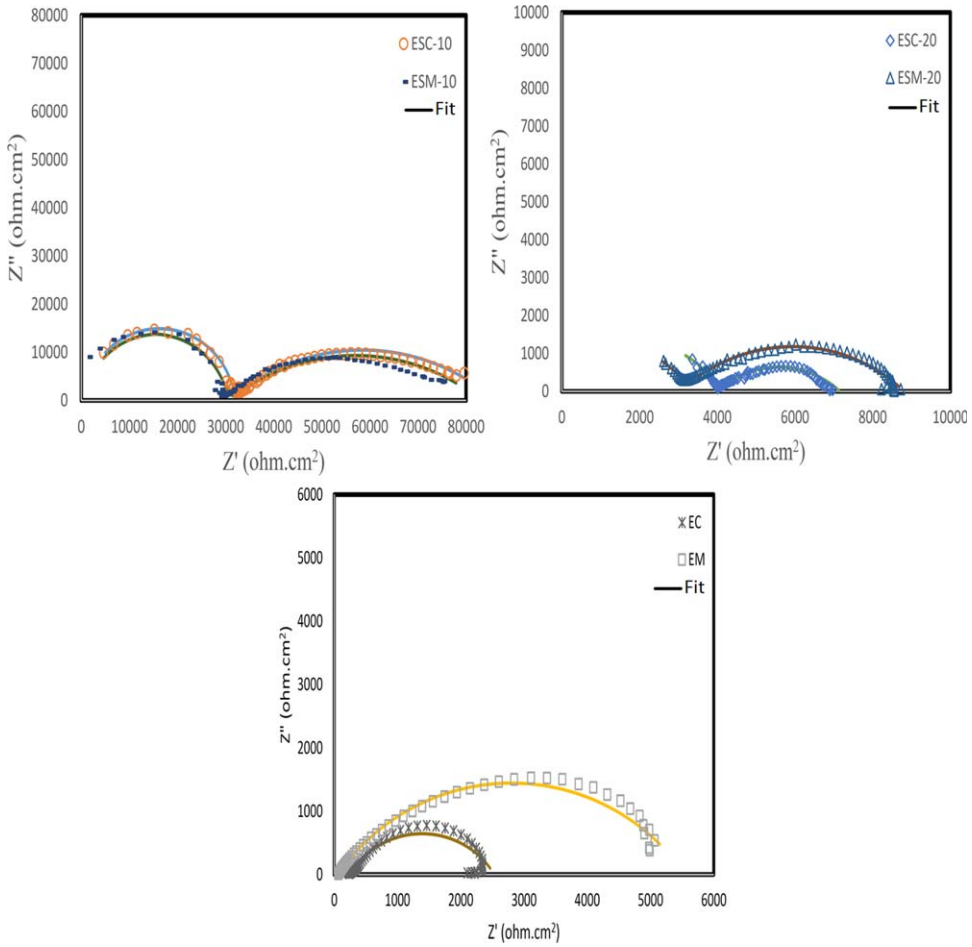

Figure 7. Nyquist plots of pure epoxy coatings and nanocomposite coatings with 10 wt % and 20 wt % SiAlON cured in oven or microwave. [Color figure can be viewed in the online issue, which is available at wileyonlinelibrary.com.]

to agglomerate as induced by their surface energy can be considered as the only reason for this event. Similar cases have been shown by Huttunen-Saarivirta *et al.*[41] that samples containing 3% halloysite have better protective performance than those with 5% halloysite. It can be deduced that SiAlON nanoparticles improve the corrosion resistance behavior for nanocomposite samples, compared to pure samples, by filling the surface defects such as nano- and microscale cracks, holes, and gaps as well as by creating blocking properties.[25] Nevertheless, the amount of added nanoparticles has an optimal value, such that samples containing 10 wt % SiAlON have greater corrosion resistance than ESC-20 and ESM-20 ones.

Electromagnetic waves have different forms. One form of them is microwaves, with a frequency about 10^{10} to 10^{12} Hz and a wavelength of about 10^{-1} to 10^{-3} m. When microwaves radiate the sample, part of them will be absorbed by the polymeric matrix and the other part will penetrate to the steel substrate. In curing with an oven, the heat will be absorbed by the surface of the sample. Therefore, the transfer of heat is done by convection, so this cure regime needs time for the heat to reach the interface of the coating and metallic substrate. A curing process by microwave starts with penetration of electromagnetic waves into the coating. The penetration of heat will stimulate all molecules of a polymeric chain. By the friction of molecules, heat will be distributed homogeneously in a coating.[47] It is obvious that in curing by oven the heating rate is slower than in the microwave regime, and these coatings were crosslinked better than coatings cured in a microwave. For this reason, the protective properties of coatings cured in an oven are slightly better than that of the other coatings.

EIS Test. Nyquist and Bode plots were used to investigate the protective performance of the pure and nanocomposite coatings. The Nyquist diagrams of coated steel samples contain two semicircles for all samples after 1 h of immersion in 3.5% NaCl (Figure 7): a small semicircle in the high-frequency range and a large semicircle in the low-frequency range. The first loop

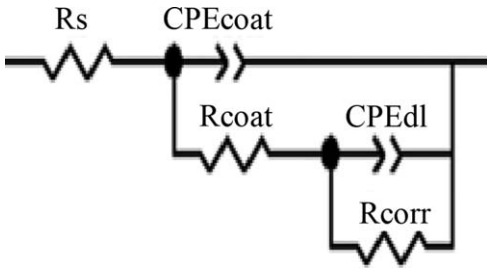

Figure 8. Equivalent electric circuit for fitting impedance data.

Table IV. Impedance Parameters Calculated by Zview2 Software

Samples	C_{coat} (F/cm^2)	R_{coat} (Ω cm^2)	C_{edl} (F/cm^2)	R_{corr} (Ω cm^2)	$\|Z\|_{0.01Hz}$	Chi-squared
ESC-10	$(3.1 \pm 0.7) \times 10^{-10}$	31321 ± 452	$(1.07 \pm 0.6) \times 10^{-5}$	54285 ± 415	81525.8 ± 1253	0.005
ESM-10	$(2.4 \pm 0.5) \times 10^{-10}$	31451 ± 354	$(1.2 \pm 0.8) \times 10^{-5}$	47463 ± 242	73941 ± 1754	0.008
ESC-20	$(6.3 \pm 0.2) \times 10^{-9}$	4178 ± 125	$(7.00 \pm 0.3) \times 10^{-5}$	3719 ± 287	7214.5 ± 627	0.003
ESM-20	$(4.1 \pm 0.4) \times 10^{-9}$	3189 ± 110	$(2.2 \pm 0.5) \times 10^{-5}$	5674 ± 157	8287.3 ± 956	0.004
EC	$(1.6 \pm 0.3) \times 10^{-5}$	314 ± 84	$(1.0 \pm 0.6) \times 10^{-4}$	2129 ± 326	2254.1 ± 356	0.005
EM	$(1.6 \pm 0.6) \times 10^{-10}$	68 ± 15	$(1.2 \pm 0.4) \times 10^{-4}$	5573 ± 672	5143.3 ± 443	0.009

characterizes the coating layer, and the second one indicates the charge transfer through the coating pores.[48–50] An electrical circuit with two time constants related to the analysis of EIS curves is shown in Figure 8. A constant phase element (CPE) was used instead of a pure capacitance in the equivalent electric circuit because of the depression in the semicircles. In the equivalent electric circuit used for fitting data, R_s, R_{corr}, R_{coat}, CPE_{coat}, and CPE_{dl} are indicative of solution resistance, charge transfer resistance, coating resistance, constant phase elements in connection with the capacitance of the coating, and constant phase elements in connection with the capacitance of the electrical double layer, respectively.[39]

Table IV summarizes the impedance parameters calculated by the Zview2 software. The values for the resistance of the coating (R_{coat}) and the low-frequency impedance ($|Z|_{0.01Hz}$) obtained after 1 h of immersion in the electrolyte solution can be used to investigate the protective performance of the coatings. The protective ability of a coating against corrosive ions can be evaluated using the coating resistance.[41] The penetration of water molecules and other corrosive ions through pores in the coating decreases by increasing the R_{coat} values, and the protective performance improved as a result.[43] As can be seen, the R_{coat} values for the ESC-10 and ESM-10 samples are higher than those of the other samples, indicating their high density and corrosion resistance compared to the pure coatings and coatings containing 20 wt % SiAlON.

The capacitance values of the coating (C_{coat}) can be used to evaluate the penetration of water into the coating.[27,48,51] Coating capacitance (C) can be derived from defined CPE values. The C values are calculated using the $CPE = 1/C(i\,\omega)^{\alpha}$ formula, where $I = -1^{1/2}$, α is a coefficient ranging between 0 and 1, and ω is the angular frequency.[27] The increase in the capacity of the coatings shows a consequent increase in the amount of water penetrating into the coating.[38] Since there is a significant difference between the dielectric constant of the organic coatings (about 4–8) and the dielectric constant of water at room temperature (about 80), a trace of water penetration into the coating leads to a relatively large change in the capacitance of the coating and results in a consequent increase in the coating capacitance.[27,52] As shown in Table IV, nanocomposite samples have much lower C_{coat} values than pure ones, which is indicative of lower water absorption by nanocomposite samples than by pure samples.[48,53] The low water absorption can be considered as a result of the high density of nanocomposite coatings such that embedding of nanoparticles decreases the free volume of the polymeric matrix. Moreover, the penetration level of aggressive ions through the microcavities in nanocomposite coatings is very low compared to that in pure coatings.[54] The results derived from the immersion and Tafel polarization tests confirm the results obtained from the EIS test. It can be noted that the amount of water absorption for samples with high coating resistance (R_{coat}) is lower than that for other samples because of the limited penetration paths in nanocomposite samples.[36,55]

Here, C_{edl} values are related to the area of the substrate in contact with the electrolyte.[27] As presented in Table IV, the ESC-10 and ESM-10 samples have lower C_{edl} values than pure samples and coatings with 20 wt % SiAlON because of the lower water-penetration values through the nanocomposite coatings. Therefore, the area of the substrate in contact with a corrosive solution for the ESC-10 and ESM-10 samples is lower than that for other samples. Besides, these samples exhibit higher resistance to corrosion than pure polymeric coatings. It is also observed that the nanocomposite samples have high R_{corr} values compared to the pure specimens, implying the high resistance of these coatings against charge transfer through the cavities and defects in the coating. The low R_{corr} value and high capacitance of the electrical double layer reveal an increase in the corroded surface area because of progressive destruction.

The corrosion resistance and total impedance of the ESC-10 and ESM-10 samples, which are higher than those of pure samples and coatings with 20 wt % SiAlON, can be obtained using the Bode plot presented in Figure 9. The low-frequency and high-frequency impedance values are associated with corrosion behavior in the coating–substrate interface and the performance of the coating in the electrolyte, respectively.[56] Therefore, the impedance values of the ESC-10 and ESM-10 samples are much higher than that of the remaining samples both at high and low frequencies, which indicates that there is a significant difference between pure and nanocomposite samples from the corrosion-resistance point of view.[24] The approximately equal impedance values for the ESC-10 and ESM-10 samples show that the type of curing regime did not have a big effect on an epoxy coating containing SiAlON nanoparticles, and both coatings exhibit almost the same corrosion-resistance behavior.

Based on the results obtained from the immersion, Tafel polarization, and EIS tests, it can be argued that SiAlON nanoparticles located in the epoxy matrix reduce the amount of water penetration. It seems that the filling of free volumes, such as

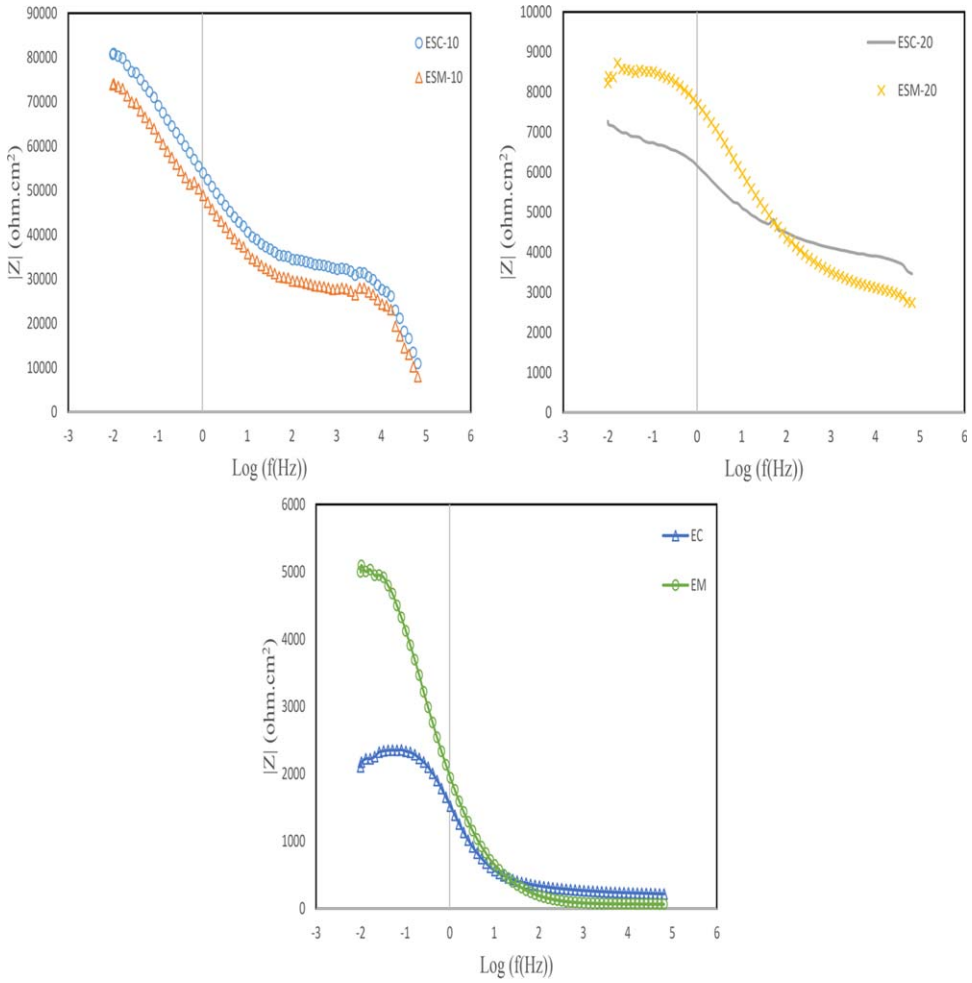

Figure 9. Bode plot for pure and nanocomposite coatings cured in oven or microwave. [Color figure can be viewed in the online issue, which is available at wileyonlinelibrary.com.]

defects and cavities in the coating, which are considered as preferred routes for penetration of corrosive agents, is among the reasons for reducing the penetration level in nanocomposite samples.[27,57] Also, SiAlON nanoparticles added to the epoxy matrix probably show barrier and blocking properties against corrosive agents,[34,58] so the penetration level of water into the interface of nanoparticles and epoxy is extremely slower than in pure epoxy. On the other hand, as previously discussed for the drop in the free volume of the coating and the decrease in the surface free energy difference between coating and substrate, the presence of nanoparticles probably leads to an increase in the strength of adhesion of the coating to the metal substrate[27]; thus, the penetration of corrosive agents into the metal substrate decreases for the case of nanocomposite samples. The decrease in the desirable effect of nanoparticles on samples containing 20 wt % SiAlON can be mainly attributed to the increase in agglomeration of the nanoparticles.

Tribological Behavior of Coatings

To evaluate the influence of embedding of SiAlON nanoparticles on the tribological properties of the coated samples, the wear resistance of the samples was investigated using the pin-on-disk wear test, as well as changes in the coefficient of friction (COF) between the coating and steel pin during the wear test. Figure 10 indicates the wear rate of various nanocomposite and pure samples cured in an oven or microwave with respect to the total weight of lost material during the wear test. As clearly shown in

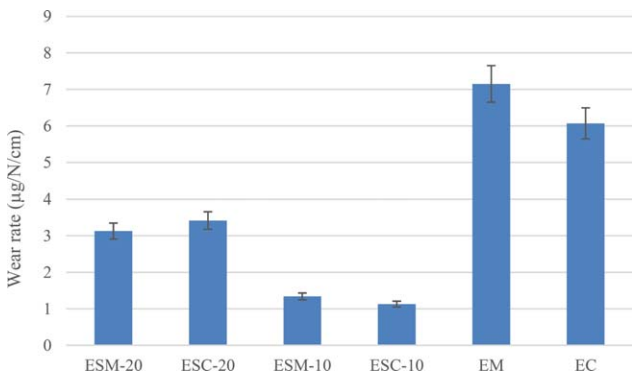

Figure 10. Curve of the overall wear values for pure and nanocomposite coatings obtained from pin-on-disk wear test. [Color figure can be viewed in the online issue, which is available at wileyonlinelibrary.com.]

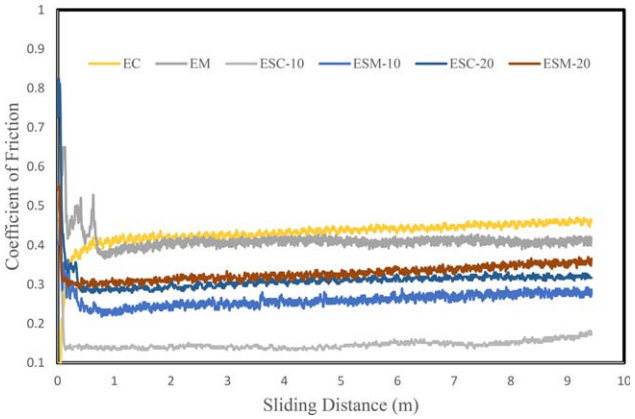

Figure 11. Curve from investigating the coefficient of friction for pure and nanocomposite coatings with 10 wt % and 20 wt % SiAlON cured in oven or microwave. [Color figure can be viewed in the online issue, which is available at wileyonlinelibrary.com.]

the figure, the wear rates for the ESC-10 and ESM-10 samples are almost five times less than that of pure samples under the same curing conditions, implying an improvement in the wear-resistance properties of the nanocomposite samples. On the other hand, the results obtained from investigating the coefficient of friction (Figure 11) show that the nanocomposite samples exhibit a lower COF than pure samples. This time, identical to the previous tests carried out to investigate the corrosion properties, it is obvious that the presence of 10 wt % nanoparticles in the epoxy matrix has a much higher impact than does 20 wt % SiAlON. Again, it can be concluded that the highest performance of nanoparticles occurs at an optimal level, and an increase in the amount of nanoparticles beyond a certain level leads to a reduction of their efficiency in terms of corrosion resistance and tribological properties.

It seems that the increase in the wear resistance of nanocomposite samples can be mainly attributed to the consequent increase in the hardness of the coating in the presence of nanoparticles.[10,11,59] Similarly, it can be concluded that the agglomeration of nanoparticles in the ESC-20 and ESM-20 samples causes a reduced effect in improving the wear-resistance properties and decreasing the coefficient of friction.[59,60] Relatively small changes of the COF for nanocomposite samples are of remarkable significance in investigating the tribological properties of these coatings. It seems that the smaller amount of abrasive particles produced in samples containing nanoparticles is among the reasons for the relative stability of the coefficient of friction during the wear process, which confirms the denser, harder, and more rigid structures of these coatings than in pure samples. The lower wear rate of nanocomposite samples can confirm the claims mentioned in the previous sections on denser structures of these coatings compared to the pure samples. Therefore, it can be concluded that the ESC-10 and ESM-10 coatings have the highest density among all the samples.

According to Hedayati *et al.*,[28] the embedding of nanoparticles (such as SiAlON) causes limited slip of the plates, reorientation, and movement of the polymer chains, leading to an increase in hardness and rigidity of the coating. Once the ratio of surface area to volume is higher, nanoparticles would show a better performance. For this reason, the agglomeration size of nanoparticles in the samples containing 20 wt % SiAlON can be guessed again. The results reveal that the presence of nanoparticles, according to the empirical equation $X_c = \eta X_p V_p + X_m V_m$, increases the hardness of the coating, where X, V, and η refer to the fraction of hardness, volume fraction, and the strengthening efficiency coefficient, respectively, and the indexes of c, p, and m represent composite, filler, and matrix, respectively.[28,61] The presence of nanoparticles in the epoxy matrix causes direct absorption by the polymeric layers of the particles.[28,62] Therefore, a strong interaction between the epoxy matrix and SiAlON nanoparticles increases the density of polymeric layers in the vicinity of the nanoparticle.[63] Since the increase in density is proportional to the increase in hardness, the rigidity and hardness of areas containing nanoparticles are higher than those of areas away from nanoparticles because of the higher density of the layers.[10] Therefore, the agglomeration of nanoparticles causes an increase in their sizes and also in the number of areas with a low density of layers, which reduces the hardness level of the coating.[28] This point is completely true in the cases of the ESC-20 and ESM-20 samples. Similar to the tests performed that are related to investigating the corrosion resistance, it can be concluded that the ESC-10 and ESM-10 samples show better wear properties than the ESC-20 and ESM-20 samples. In this case, it can be seen that the curing type does not have a considerable effect on the tribological properties of the coating. However, the highest impact on the tribological properties of the coating samples is related to the number of dispersed nanoparticles.[10] Nanoparticles located in the polymer matrix should not be agglomerated because their performance decreases.

CONCLUSIONS

SiAlON nanoparticles have a significant impact on improving the corrosion protection and wear-resistance performance of the nanocomposite coatings if they are embedded properly into the epoxy matrix. Embedding of nanoparticles causes the filling of the free volumes in the coating, providing barrier and blocking properties against corrosive agents. In addition, it leads to the creation of harder, more rigid, and relatively denser structures compared with pure samples. The corrosion rate of ESC-10 and ESM-10 coatings is 15 to 18 times lower than that of pure epoxy samples. The ESC-20 and ESM-20 samples had weak corrosion resistance and tribological properties compared to the samples containing 10 wt % SiAlON because of the increase in agglomeration level of nanoparticles during the dispersion process.

The crystallization and strength of the chains produced after either oven or microwave curing operations were almost equal to each other. In addition, coatings produced under similar conditions indicated similar linking densities and exhibit almost similar protective behaviors in terms of corrosion protection and tribological performance.

REFERENCES

1. Min, S.; Polycarpou, A. A. *Tribol. Int.* **2013**, *60*, 198.
2. Bilyeu, B.; Brostow, W.; Menard, K. P. *J. Mater. Educ.* **1999**, *21*, 281.
3. Bilyeu, B.; Brostow, W.; Menard, K. P. *J. Mater. Educ.* **2000**, *22*, 107.
4. Bilyeu, B.; Brostow, W.; Menard, K. P. *J. Mater. Educ.* **2001**, *23*, 189.
5. Gaury, J.; Kelder, E. M.; Bychkov, E.; Biskos, G. *Thin Solid Films* **2013**, *534*, 32.
6. Hwang, K. S.; Jeon, Y. S.; Hwangbo, S.; Kim, J. T. *Ceram. Int.* **2013**, *39*, 8555.
7. Malucelli, G.; Gianni, A.; Deflorian, F.; Fedel, M.; Bongiovanni, R. *Corros. Sci.* **2009**, *51*, 1762.
8. Zhou, C.; Lu, X.; Xin, Z.; Liu, J.; Zhang, Y. *Corros. Sci.* **2014**, *80*, 269.
9. Rout, T. K.; Gaikwad, A. V. *Prog. Org. Coatings* **2015**, *79*, 98.
10. Myshkin, N. K.; Petrokovets, M. I.; Kovalev, A. V. *Tribol. Int.* **2006**. *38*, 910.
11. Brostow, W.; Kovačevic, V.; Vrsaljko, D.; Whitworth, J. *J. Mater. Educ.* **2010**, *32*, 273.
12. Alamri, H.; Low, I. M. *Mater. Des.* **2012**, *42*, 214.
13. Palraj, S.; Selvaraj, M.; Maruthan, K.; Rajagopal, G. *Prog. Org. Coatings* **2015**, *81*, 132.
14. Piazza, D.; Lorandi, N. P.; Pasqual, C. I.; Scienza, L. C.; Zattera, A. *J. Mater. Sci. Eng. A* **2011**, *528*, 6769.
15. Liu, X. J. *Mater. Res. Bull.* **2003**, *38*, 1939.
16. Gong, X. *Ceram. Int.* **2014**, *40*, 7161.
17. Ahmadi, Z.; Nayebi, B.; Shahedi Asl, M.; Ghassemi Kakroudi, M. *Mater. Charact.* **2015**, *110*, 77.
18. Sabagh, S.; Bahramian, A. R.; Kokabi, M. *Iran. Polym. J.* **2012**, *21*, 837.
19. Celik, A.; Lazoglu, I.; Kara, A.; Kara, F. *J. Mater. Process. Technol.* **2015**, *223*, 39.
20. Tu, G.; Wu, S.; Liu, J.; Long, Y.; Wang, B. *Int. J. Refract. Met. Hard Mater.* **2016**, *54*, 330.
21. Lu, D.; Pan, S. *Polym. Eng. Sci.* **2006**, *46*, 820.
22. Koo, C. M.; Ham, H. T.; Choi, M. H.; Kim, S. O.; Chung, I. *J. Polymer (Guildf)* **2003**, *44*, 681.
23. Ranganatha, S.; Venkatesha, T. V.; Vathsala, K. *Appl. Surf. Sci.* **2010**, *256*, 7377.
24. Shahri, Z.; Allahkaram, S. R. *Iran. Mater. Sci.* **2012**, *10*, 49-57.
25. Mazaheri, H.; Allahkaram, S. R. *Appl. Surf. Sci.* **2012**, *258*, 4574.
26. Zamanizadeh, H. R.; Shishesaz, M. R.; Danaee, I.; Zaarei, D. *Prog. Org. Coatings* **2015**, *78*, 256.
27. Mirabedini, S. M.; Thompson, G. E.; Moradian, S.; Scantlebury, J. D. *Prog. Org. Coatings* **2003**, *46*, 112.
28. Hedayati, M.; Salehi, M.; Bagheri, R.; Panjepour, M.; Naeimi, F. *Prog. Org. Coatings* **2012**, *74*, 50.
29. Hosseini, M. G.; Jafari, M.; Najjar, R. *Surf. Coat. Technol.* **2011**, *206*, 280.
30. Hosseini, M. G.; Raghibi-Boroujeni, M.; Ahadzadeh, I.; Najjar, R.; Seyed Dorraji, M. S. *Prog. Org. Coatings* **2009**, *66*, 321.
31. Zhang, G.; Liao, H.; Cherigui, M.; Davim, J. P.; Coddet, C. *Eur. Polym. J.* **2007**, *43*, 1077.
32. Behzadnasab, M.; Mirabedini, S. M.; Esfandeh, M. *Corros. Sci.* **2013**, *75*, 134.
33. Kisin, S. Ph.D. Thesis, Department of Chemical Engineering and Chemistry, Eindhoven University of Technology, **2007**.
34. Mayne, J. E. O.; Scantlebury, J. D. *Br. Polym. J.* **1971**, *3*, 237.
35. Misev, T. A. Powder Coatings: Chemistry and Technology; John Wiley & Sons: Hoboken, NJ, **1991**.
36. Bagherzadeh, M. R.; Mahdavi, F. *Prog. Org. Coatings* **2007**, *60*, 117.
37. Mansfeld, F.; Kendig, M. W.; Tsai, S. *Corrosion* **1982**, *38*, 478.
38. Naderi, R.; Attar, M. M.; Moayed, M. H. *Prog. Org. Coatings* **2004**, *50*, 162.
39. Ćirić-Marjanović, G. N.; Marjanović, B. N.; Popović, M. M.; Panić, V. V.; Mišković-Stanković, V. B. *Russ. J. Electrochem.* **2006**, *42*, 1358.
40. Mišković-Stanković, V. B.; Stanić, M. R.; Dražić, D. M. *Prog. Org. Coatings* **1999**, *36*, 53.
41. Huttunen-Saarivirta, E.; Vaganov, G. V; Yudin, V. E.; Vuorinen, J. *Prog. Org. Coatings* **2013**, *76*, 757.
42. Yeh, J. M. *Polymer (Guildf)* **2002**, *43*, 2729.
43. Mostafaei, A.; Nasirpouri, F. *Prog. Org. Coatings* **2014**, *77*, 146.
44. Liu, D. *Colloids Surf. A* **2015**, *472*, 85.
45. Yang, X. et al. *J. Solid State Electrochem.* **2010**, *14*, 1601.
46. Saji, V. S.; Thomas, J. *Curr. Sci.* **2007**, *92*, 51.
47. Das, S.; Mukhopadhyay, A. K.; Datta, S.; Basu, D. *Bull. Mater. Sci.* **2008**, *31*, 943.
48. Ashassi-sorkhabi, H.; Seifzadeh, D. *Arab. J. Chem.* **2012**.
49. Bakhshandeh, E.; Jannesari, A.; Ranjbar, Z.; Sobhani, S.; Saeb, M. R. *Prog. Org. Coatings* **2014**, *77*, 1169.
50. Jones, D. A. Principles and Prevention of Corrosion, 2nd ed.; Pearson, **1996**.
51. Pramoda, K. P.; Liu, T.; Liu, Z.; He, C.; Sue, H. *J. Polym. Degrad. Stab.* **2003**, *81*, 47.
52. Brasher, D. M.; Kingsbury, A. H. *J. Appl. Chem.* **1954**, *4*, 62.
53. Deflorian, F.; Fedrizzi, L.; Rossi, S.; Bonora, P. L. *Electrochim. Acta* **1999**, *44*, 4243.
54. Richardson, J. A.; Wood, G. C. *Corros. Sci.* **1970**, *10*, 313.
55. Leidheiser Jr, H.; Granata, R. D. *IBM J. Res. Dev.* **1988**, *32*, 582.
56. Shao, F. *Surf. Coat. Technol.* **2015**, *276*, 8.
57. Grundmeier, G.; Schmidt, W.; Stratmann, M. *Electrochim. Acta* **2000**, *45*, 2515.

58. Yin, Y.; Liu, T.; Chen, S.; Liu, T.; Cheng, S. *Appl. Surf. Sci.* **2008**, *255*, 2978.
59. Zhang, M. Q.; Rong, M. Z.; Luo, Y. *Polym. Compos.* **2005**, *13*, 245.
60. Luo, Y.; Rong, M. Z.; Zhang, M. Q. *Polym. Polym. Compos.* **2005**, *13*, 245.
61. Hussain, F.; Hojjati, M.; Okamoto, M.; Gorga, R. E. *J. Compos. Mater.* **2006**, *40*, 1511.
62. Tadd, E.; Zeno, A.; Zubris, M.; Dan, N.; Tannenbaum, R. *Macromolecules* **2003**, *36*, 6497.
63. Vollenberg, P. H. T.; Heikens, D. *Polymer (Guildf)* **1989**, *30*, 1656.